**11**

# A Scalable Healthcare Integrated Platform (SHIP) and Key Technologies for Daily Application

Wenxi Chen, Xin Zhu, Tetsu Nemoto[1], Daming Wei and Tatsuo Togawa[2]
*Biomedical Information Technology Lab., the University of Aizu*
*[1]School of Health Sciences, Faculty of Medicine, Kanazawa University*
*[2]School of Human Sciences, Waseda University*
*Japan*

## 1. Introduction

A ubiquitous era has arisen based on achievements from the development of science and technology over the previous 1,000 years, and especially the past 150 years. Among the numerous accomplishments in human history, four fundamental technologies have laid the foundation for today's pervasive computing environment.

The electromagnetic wave theory, established by James Maxwell in 1864, predicted the existence of waves of oscillating electric and magnetic fields that travel through empty space at a velocity of 310,740,000 m/s. His quantitative connection between light and electromagnetism is considered one of the great triumphs of 19th century physics. Twenty years later, through experimentation, Heinrich Hertz proved that transverse free space electromagnetic waves can travel over some distance, and in 1888, he demonstrated that the velocity of radio waves was equal to the velocity of light. However, Hertz did not realize the practical importance of his experiments. He stated that, "It's of no use whatsoever … this is just an experiment that proves Maestro Maxwell was right – we just have these mysterious electromagnetic waves that we cannot see with the naked eye. But they are there." His discoveries were later utilized in wireless telegraphy by Guglielmo Marconi, and they formed a part of the new "radio communication age".

The second fundamental technology is spread-spectrum telecommunications, whose multiple access capability allows a large volume of users to communicate simultaneously on the same frequency band, as long as they use different spreading codes. This has been developed since the 1940s and used in military communication systems since the 1950s. Realization of spread-spectrum technology requires a large computational capacity and leads to a bulky size and weight. Since the initial commercial use of spread spectrum telecommunications began in the 1980s, it is now widely used in many familiar systems today, such as GPS, Wi-Fi, Bluetooth, and mobile phones. This was made possible by the invention of computing machines and integrated circuits, the third and fourth tremendous triumphs.

The first automatic computing machine, known as ENIAC, was built using 18,000 vacuum tubes, 1,500 relays, 70,000 resistors, and 10,000 condensers. It performed 35,000 additions per

second and cost US$487,000 (Nohzawa, 2003). The latest CPU, the Yorkfield XE, contains 820 million transistors on $2 \times 107$ mm² dies and features a 1333 MT/s FSB and a clock speed of 3 GHz (Intel Corp., 2007).

Since the first integrated circuit (IC), which contained a single transistor and several resistors on an $11 \times 1.6$ mm² germanium chip, was fabricated by Jack Kilby in 1958, advanced 45 nm semiconductor technology makes it possible to condense an entire complicated spread-spectrum telecommunication system into a magic box as small as a mobile phone.

Today, we are interconnected through wired and wireless networks, and surrounded by an invisible pervasive computing environment. This makes "information at your fingertips" and "commerce at light speed" possible. We are already acclimatized to enjoy everything worldwide conveniently, wherever we are. We enjoy online shopping and share information with friends from the other side of the Earth in an instant.

However, this is a double-edged sword. Our daily lifestyle has changed dramatically. While we may benefit from the advantages of today's society, at the same time, we face many unprecedented problems in the health domain, which have emerged with all of these changes.

One of the greatest concerns is the ascent of chronic illness that has occurred concurrently with the accompanying lifestyle changes. Figure 1 shows the change in mortality among different diseases from acute to chronic over the past 100 years in Japan. There has not been a large change in conventional causes of death, such as contingency, caducity, and pneumonia. Acute infectious diseases, such as tuberculosis, have disappeared completely since the 1980s. However, death due to chronic conditions is increasing. The leading causes of death are the three "C" top killer diseases: cerebral, cardiovascular, and cancer (malignant neoplasm), which account for 60 per cent of total deaths.
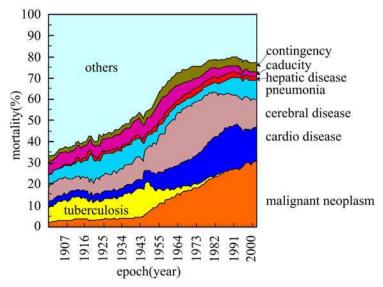


Fig. 1. Change in mortality of different diseases over the previous century in Japan. (Adapted from the Japanese Ministry of Health, Labour, and Welfare).

Rapid changes in both societal environment and daily lifestyle are responsible for most of these chronic illnesses. Treatment of chronic conditions is now recognized as a problem of all society and no longer just a private issue. To elevate all citizens' awareness of the importance of health promotion and disease prevention in response to the steep increase in long-term healthcare requirements, it is indispensable to be involved in every aspect and to take creative action. A variety of innovative strategies and activities are now being explored nationwide in Japan at three levels: macro (administration), meso (community, organization, and company), and micro (personal) levels.

At the macro level, a 12-year health promotion campaign, known as "Healthy Japan 21" (Japan Health Promotion and Fitness Foundation, 2000), has been advocated nationwide since 2000 and is financially supported by the Japanese Ministry of Health, Labour, and Welfare. Furthermore, a "health promotion law" (Japanese Ministry of Health, Labour and Welfare, 2002) was issued by the Japanese parliament. This reconfirmed that the national goal of medical insurance reconstruction was health promotion and disease prevention, and it defined individual responsibility and coordination among citizens, community, and government organizations.

At the meso level, industrial organizations and research institutions have developed many Internet-based systems and related devices for daily healthcare. Professional organizations and academic associations have established a series of educational programs and accreditation systems for professional healthcare promoters. Citizen communities have boosted health promotion campaigns through various service options.

At the micro level, more and more people are aware of the importance of health promotion and chronic prevention, and are becoming more active in participating in daily personal healthcare practices. They spend a lot of time and money on exercise, diet, and regular medical examinations to keep their biochemical indices as good as possible.

This trend turns out that in the US only, the healthcare domain is now growing up into a giant industrial territory worthy of about US$2 trillion annually (MarketResearch.com. 2008). In terms of building a better healthcare environment, and as one of the initiatives in the arena of human welfare in long-term chronic treatment, we are confronting the challenges of providing effective means for vital sign monitoring technologies suitable for daily use, and large-scale data mining and a comprehensive interpretation of their physiological interconnection. These solutions are being developed across the world. Many companies are already engaged in and placing priority on, providing a total solution to these ever-increasing demands.

The "Health Data Bank" ASP service platform was released as a multifaceted aid for the health management of corporate employee medical exam results (NTT Data Corp., 2002). The service supplies healthcare personnel with a set of tools for effective employee health guidance and counselling, and takes into account factors such as an employee's current physical condition, as well as living habits and environment, and age-related changes in longitudinal management in accumulated individual data. Individual corporate employees can browse their personal data through Internet channels, and view records of their check-ups, as well as graphs detailing historical changes in their health condition, thus facilitating improved personal health management.

Companies and research institutes in the European Union have launched several multinational projects to develop wearable and portable healthcare systems for personalized care. The "MyHeart" project is a framework for personal healthcare applications led by Philips, which aims to develop on-body sensors/electronics and appropriate services to help

fight cardiovascular disease through prevention and early diagnosis. It can monitor vital signs and physical movement via wearable textile technology, process the measured data, and provide the user with recommendations (Philips Electronics, 2004). After the completion of the "MyHeart" program, a continuation "HeartCycle" project began in March 2008. Many new sensors and key technologies, such as a cuff-less blood pressure sensor, a wearable SpO2 sensor, an inductive impedance sensor, an electronic acupuncture system, a contactless ECG, arrays of electret foils, a motion-compensation system for ECG, and a cardiac performance monitor (from bioimpedance) will be developed and built into the system. A patient's condition will be monitored using a combination of unobtrusive sensors built into the patient's clothing or bed sheets and home appliances, such as weighing scales and blood pressure meters. Data mining and decision support approaches will be developed to analyse the acquired data, to predict the short-term and long-term effects of lifestyle and medication, and to obtain an objective indicator of patient compliance (Philips Electronics, 2008).

"MobiHealth" was a mobile healthcare project funded by the European Commission from 2002 to 2004. Fourteen partners from hospitals and medical service providers, universities, mobile network operators, mobile application service providers, mobile infrastructure, and hardware suppliers across five European countries participated in the project. It allowed patients to be fully mobile while undergoing health monitoring without much discomfort in daily activities. The patients wore a lightweight unit with multiple sensors connected via a Body Area Network (BAN) for monitoring ECG, respiration, activity/movement/position, and a plethysmogram over short or long periods with no need to stay in hospital (European Commission, 2002).

The "AMON" system was designed to monitor and evaluate human vital signs, such as heart rate, two-lead ECG, blood pressure, oxygen blood saturation, skin perspiration, and body temperature using a wrist-mounted wearable device. The device gathers the data and transmits it to a remote telemedicine centre for further analysis and emergency care, using a GSM/UMTS cellular infrastructure (Anliker et al., 2004; European Commission, 2001).

"HealthVault" aims to build a universal hub of a network to connect personal health devices and other services that can be used to help store, and manage personal medical information in a single central site on the Web (Microsoft Corp., 2008). It will provide a seamless connection interface scheme for various home health and wellness monitoring devices, such as sport watches, blood glucose monitors, and blood pressure monitors marketed by medical equipment manufacturers worldwide.

On the other hand, many explorative studies on fundamental technology for vital signs monitoring have been conducted in the academic world and in research institutes. Much innovative instrumentation suitable in daily life has emerged and is gradually being commercialized.

Since the first accurate recording of an ECG reported by Willem Einthoven in 1895, and its development as a clinical tool, variants, such as Holter ECG, event ECG, and ECG mapping are now well known and have found a variety of applications in clinical practice. Measurement of ECG is now available from various scenarios. Whenever a person sits on a chair (Lim et al., 2006) or on a toilet (Togawa et al., 1989), sleeps in a bed (Kawarada et al., 2000; Ishijima, 1993), sits in a bathtub (Mizukami et al., 1989; Tamura et al., 1997), or even takes a shower (Fujii et al., 2002), his/her heart beat can be monitored, with the person unaware.

The smart dress, "Wealthy outfit", weaves electronics and fabrics together to detect the wearer's vital signs, and transmits the data wirelessly to a computer. The built-in sensors

gather information on the wearer's posture and movement, ECG, and body temperature. Despite having nine electrodes and conductive leads woven into it, the suit looks and feels completely normal (Rossi et al., 2008; Marculescu et al., 2003).

The wellness mobile phone, "SH706iw", manufactured by the Sharp Corp. (Japan), has been released by NTT DoCoMo Corp. (Japan) in September 2008. It will have all the standard features of a mobile phone but will also act as a pedometer, a body fat meter, a pulse rate, and a breath gas monitor. Moreover, a built-in game-like application will support daily health management for fun and amusement (Sharp Corp., 2008; DoCoMo Corp., 2008).

According to an investigation report from the World Health Organization (WHO, 2002), most current healthcare systems still have some common issues that need to be addressed. (a) The difference between acute and chronic care is not sufficiently emphasized. The overall concept in system development has not shifted enough towards chronic conditions, and has not evolved to meet this changing demand. (b) Despite the importance of patients' health behaviour and adherence to improvement for chronic conditions, patients are not provided with a simple way to involve themselves in self-management and to have essential information to handle their condition to the best extent possible. (c) Patients are often followed up sporadically, and are seldom provided with a long-term management plan for chronic conditions to ensure the best outcomes.

Indeed, they are large obstacles in front of us that need to be cleared. We consider these issues a long-term difficult challenge to governments, communities, and individuals alike. We deem two main aspects should be paid primary attention. The first aspect is that vital-sign monitoring for chronic conditions requiring different philosophy and strategy tends to be ignored. Long-term chronic care is mostly oriented to untrained users in the home environment. However, many devices are far from being "plug and play", and require tedious involvement in daily operation. The second aspect is the lack of interconnection between multifarious physiological data within existing medical systems, as medication is usually decided by interpretation based on fragmented data and standards based on acute and emergent symptoms, and is often provided without the benefit of complete long-term physiological data.

To meet current needs, and to tackle the two problems above, our studies focus on developing a series of wearable/invisible vital-sign measurement technologies to facilitate data collection in the daily environment in perpetuity, and on applying data mining algorithms to conduct comprehensive interpretation of multifarious long-term data fusion, and ultimately to build a scalable healthcare integrated platform, SHIP, for various applicable domains, wherever vital signs are conducive.

## 2. Methods and results

Our studies included developing a series of instrumental technologies and data mining mathematical algorithms to construct finally a versatile platform, SHIP, integrated with wired and wireless network technologies. The following paragraphs describe an overall vision of SHIP and introduce three related constitutional technologies that we have been developing since 2002 (Chen et al., 2004).

### 2.1 SHIP

SHIP was conceived to provide three functions: (a) detection (monitoring multifarious vital signs by wearable/invisible means, (b) analysis (comprehensive interpretation of long-term

physiological data using data mining mathematics), and (c) service (providing customizable services to various human activity fields by a combination of multiple key technologies).

As shown in Fig. 2, SHIP was constructed in a three-layer model which was supported by five pillars and many bricks.

| elderly | active senior | health insurer | fitness gym | pharmaceutical house | public institution | target |
|---|---|---|---|---|---|---|
| EBC | EBH | EBI | EBE | EBT | EBS | service |
| Scalable Healthcare Integrated Platform (SHIP) | | | | | | platform |

| | | |
|---|---|---|
| Internet - global wired connection | | communication & management |
| Mobile Phone - global wireless connection | | |
| Bluetooth - short range wireless connection | | |
| Data Mining Mathematics - comprehensive exploitation of long-term & large scale physiological data | | analysis |
| Wearable and Invisible Measurement - ubiquitous monitoring of vital signs (wake or sleep, indoor or outdoor) | | detection |

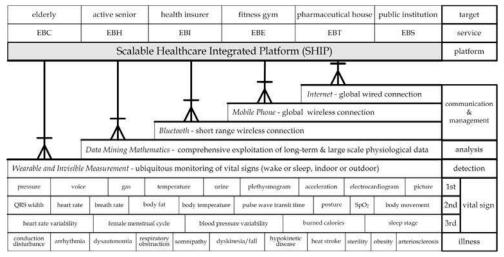| pressure | voice | gas | temperature | urine | plethysmogram | acceleration | electrocardiogram | picture | 1st | |
|---|---|---|---|---|---|---|---|---|---|---|
| QRS width | heart rate | breath rate | body fat | body temperature | pulse wave transit time | posture | SpO2 | body movement | 2nd | vital sign |
| heart rate variability | | female menstrual cycle | | blood pressure variability | | burned calories | | sleep stage | 3rd | |
| conduction disturbance | arrhythmia | dysautonomia | respiratory obstruction | somnipathy | dyskinesia/fall | hypokinetic disease | heat stroke | sterility | obesity | arteriosclerosis | illness |

Fig. 2. Systemic architecture of the scalable healthcare integrated platform is founded on bricks, and supported by five pillars in a three layers structure. A variety of application domains can be created using the SHIP.

The first layer consists of a series of bricks for physiological data detection in three orders. Each brick in the first order can be considered as being a wearable/invisible measurement method, which can be used either indoors or outdoors, either awake or asleep. While each brick in the second and third orders indicates a data mining approach to derive information from the other bricks. The direct measurement signals are denoted as first-order vital signs. Second-order vital signs, such as heart rate, are derived from the first-order parameters. Third-order signs originate from the first- and second-order parameters.

Some of direct measurement objects are: pressure, voice, gas, temperature, ECG, acceleration, plethysmogram, and urine. The second-order vital signs are derived from the first-order vital signs, such as the QRS width and heart rate from ECG, the pulse rate and breathing rate from the pressure (Chen et al., 2005), posture and body movement from acceleration (Zhang et al., 2007), and pulse wave transit time from the ECG and plethysmogram. The third-order vital signs are derived from both the second-order and the first-order vital signs. For example, the variability in heart rate is derived from the heart rate profile. The female menstrual cycle is estimated from the body temperature (Chen et al., 2008a), and the variation in blood pressure is estimated from the pulse wave transit time (Chen et al., 2000). Changes in these parameters are indicators of specific ailments, such as arrhythmia from the variability in heart rate, somnipathy from body movements and sleep stage, and respiration obstruction from SpO2. We combined the directly measured and derived parameters to treat related illnesses such as cardiovascular disease, obesity, and respiratory obstruction.

Data mining mathematics for data analysis resides in the second layer. Most of statistical approaches and data warehouse technologies are applicable to conduct a comprehensive exploitation of the large volume of long-term accumulated physiological data. Innovative findings and understanding from this layer will be one of five pillars to support various application domains.

The third layer consists of three pillars and is responsible for data communication and management through wireless and wired networking technology. Bluetooth telemetry technology is adopted as one pillar to support short-range wireless communication of data between sensor devices and home units or mobile phones. Mobile telephony and the Internet are two other pillars and used for wide-range data telecommunication and management.

SHIP has four characteristic features. (a) Its ubiquity makes it possible to detect and collect vital signs either asleep (unconscious status) or awake (conscious status), and either outdoors or indoors through wearable/invisible measurements and wired or wireless networks. (b) Its scalability allows users to customize their special package to meet individual needs, and also service providers to match different requests from medical/clinical use, industries, government agencies, and academic organizations through a variety of partnership options. (c) Its hot-line connectivity is realized by either mobile telephony or Internet (indoors or outdoors) and guarantees that any emergent event can be captured and responded to in real time. (d) Its interoperability is provided through a data warehouse that is configured in two formats. An exclusive format maintains security and enables high-speed data transmission within SHIP, and an externally accessible format ensures that SHIP is open to other allied systems through the HL7 standard (Health Level Seven Inc., 1997) to provide a seamless interface that is compatible with other existing medical information systems.

SHIP is intended to create a flexible platform for the exchange, management, and integration of long-term data collected from a wide spectrum of users, and to provide various evidence-based services to diverse domains. Subjects in target services are not only elderly and active seniors in healthcare but also subjects such as pharmaceutical houses for therapeutic effect tracing, insurance companies involved in risk assessment and claim transactions, transportation system drivers, fire fighters, and policemen involved in public security.

The layer and brick model in the SHIP architecture makes it possible to integrate many elementary achievements from ourselves and co-workers. Three different types of fundamental instrumentation (invisible/wearable/ubiquitous) and the results of data mining from our studies are introduced in the following sections.

## 2.2 Invisible sleep monitor

Invisible measurement means that a sensor unit can be deployed in an unoccupied area and is unobtrusive and concealable. Monitoring of vital signs can be performed in an invisible way, such that a user is unaware of its existence and does not have to take care that the device is present at all.

A schematic illustration of invisible sleep monitoring is shown in Fig. 3. There is a sensor plate and a bedside unit in the system configuration. A sensor unit is placed beneath a pillow, which is stuffed with numerous fragments of soft comfortable materials formed from synthetic resins. Two incompressible polyvinyl tubes, 30 cm in length and 4 mm in diameter, are filled with air-free water preloaded to an internal pressure of 3 kPa and set in

parallel at a distance of 11 cm from each other. A micro tactile switch (B3SN, Omron Co. Ltd) is fixed along the central line between the two parallel tubes. The two tubes above and the micro switch are sandwiched between two acrylic boards, both 3 mm thick. One end of each tube is hermetically sealed and the other end is connected to a liquid pressure sensor head (AP-12S, Keyence Co. Ltd). The inner pressure in each tube includes static and dynamic components, and changes in accordance with respiratory motion and cardiac beating. The static pressure component responds to the weight of the user's head, and acts as a load to turn on a micro tactile switch. The dynamic component reflects the weight fluctuation of the user's head due to breathing movements and pulsatile blood flow from the external carotid arteries around the head. Pressure signals beneath the near-neck and far-neck occiput regions are amplified and band-pass filtered (0.16–5 Hz), and the static component is removed from the signal. Only the dynamic component is digitized at a sampling rate of 100 Hz and transmitted to a remote database server through an Internet connection. The tactile switch is pressed to turn on a DC power supply via a delay switch (4387A-2BE, Artisan Controls Corp.) when the user lies down to sleep and places his/her head on the pillow.
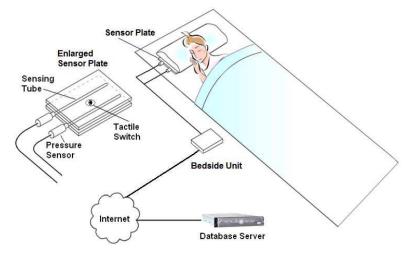


Fig. 3. Schematic illustration of the invisible monitoring of vital signs during sleep. A sensor plate is placed beneath a pillow. Signals reflecting pressure changes under the pillow are detected, digitized, and transmitted to a database server via the Internet by a bedside unit.

A 60 s fragment of raw signal measured under the near-neck occiput region during sleep is shown in Fig. 4(a). The breathing rate (BR), heart rate (HR), and body movements can be detected from the raw data measurements.

The BR and HR are detected by wavelet transformation on a dyadic grid plane using a multiresolution procedure, which is implemented by a recursive à trous algorithm. The Cohen–Daubechies–Fauraue (CDF) (9, 7) biorthogonal wavelet is the basis function used to design the decomposition and reconstruction filters (Daubechies, 1992). The raw measured signal is decomposed into an approximation and multiple detailed components through a cascade of filter banks (Mallat & Zhong, 1992; Shensa, 1992). Further mathematical theories can be found in Daubechies, 1992 and Akay, 1998. Implementation details are given in Chen et al., 2005, and Zhu et al., 2006.

The wavelet transformation (WT) of a signal, $x(t)$, is defined as follows:

$$W_s x(t) = \frac{1}{s} \int_{-\infty}^{+\infty} x(\tau) \psi(\frac{t-\tau}{s}) d\tau \ , \tag{2-2-1}$$

where $s$ is the scale factor and $\psi(t)$ is the wavelet basis function. This is called a dyadic WT if $s = 2^j$ ( $j \in Z$ and $Z$ is the integral set). Two filter banks, the low-pass and high-pass decomposition filters $\mathbf{H}_0$ and $\mathbf{H}_1$, and associated reconstruction filters, $\mathbf{G}_0$ and $\mathbf{G}_1$, can be derived from the wavelet basis function and its scaling function, respectively. Using Mallat's algorithm, the dyadic WT of the digital signal, $x(n)$, can be calculated as follows:

$$A_{2^j} x(n) = \sum_{k \in Z} h_{0,2n-k} A_{2^{j-1}} x(k) \ , \tag{2-2-2}$$

$$D_{2^j} x(n) = \sum_{k \in Z} h_{1,2n-k} A_{2^{j-1}} x(k) \ , \tag{2-2-3}$$

where $A_{2^j} x(n)$ and $D_{2^j} x(n)$ are the approximation and detail components, respectively, in the $2^j$ scale, and $x(n)$ (or $A_{2^0} x(n)$) is the raw data signal. The terms $h_0$ and $h_1$ are the filter coefficients of $\mathbf{H}_0$ and $\mathbf{H}_1$, respectively. Therefore, $A_{2^j} x(n)$ and $D_{2^j} x(n)$ (j∈Z) can be extracted from $x(n)$ (or $A_{2^0} x(n)$) using equations (2-2-2) and (2-2-3) recursively. The $2^{j-1}$ scale approximation signal can also be reconstructed from the $2^j$ scale approximation and the detail component:

$$\hat{A}_{2^{j-1}} x(n) = \sum_{k \in Z} g_{0,n-2k} A_{2^j} x(k) + \sum_{k \in Z} g_{1,n-2k} D_{2^j} x(k) \ , \tag{2-2-4}$$

where $g_0$ and $g_1$ are the filter coefficients of $\mathbf{G}_0$ and $\mathbf{G}_1$, respectively. The terms $\hat{x}(n)$ (or $\hat{A}_{2^0} x(n)$) can be finally reconstructed by repeatedly using equation (2-2-4). Any noise in $D_{2^j} x(n)$ can be removed using a soft or hard threshold method before $\hat{A}_{2^{j-1}} x(n)$ is reconstructed. It should be pointed out that the sampling rate of the $2^j$ scale approximation and detail is $f_s / 2^j$, where $f_s$ is the sampling rate of the raw signal.

Because the $2^6$ scale approximation waveform is close to a human breathing rhythm, while the detail waveforms of both the $2^4$ and $2^5$ scales contain peaks similar to those of human heartbeats, the $2^6$ scale approximation component, A6, is used to reconstruct the waveform for obtaining the BR, and the D4 and D5 detail components at the $2^4$ and $2^5$ scales are combined into a single synthesized waveform and then reconstructed to detect the HR. Figure 4(b) shows the reconstructed waveforms for HR detection, and Fig. 4(c) shows the reconstructed waveforms for BR detection.

During a night's sleep, over a period of 4–8 h, a regular pulsation due to either the heart beating or breathing is not always detectable. Body movements may greatly distort the pressure variation signal pattern. In such a time slot, either the BR or the HR, and sometimes even both, are barely detectable. Instead, body movements are detected using a statistical method in such time slots. If a very large change, whose absolute value is four times larger than the standard deviation of the preceding detected movement-free raw

signal, is detected in the incoming signal, the preceding and succeeding 2.5 s periods from the movement detection point are treated as being body movement periods and not used to estimate the BR and HR. Detection of the BR is more sensitive to body movements than detection of the HR is.
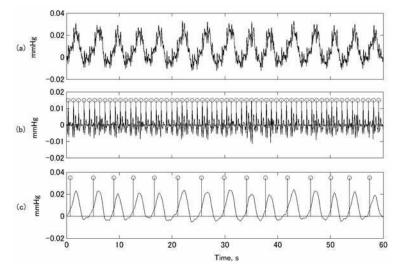


Fig. 4. A body movement-free sample and the detected BR and HR beat-by-beat. (a) The raw pressure signal data measured under the near-neck occiput region. (b) The pulse-related waveform reconstructed from the D4 and D5 components. (c) The breath-related waveform reconstructed from the A6 component. The open circles indicate the detected characteristic points for BR/HR determination.

Figure 5(a) shows a 60 s segment of a raw signal, which includes body movement during unstable sleep. When the pressure signal is distorted by a body movement, the periods detected that are from two reconstructed waveforms (HR-related and BR-related) are not always identical in both time and length. Because HR detection is usually more robust than BR detection, body movement detection from reconstructed BR-related waveforms is longer than that from HR-related waveforms. The final body movement outcome is an OR operation of both results. In the case shown in Fig. 5, the body movement period in terms of HR-related waveform detection is counted as 15.4 s, while that in terms of BR is 35.9 s. The final body movement outputs as 37.8 s from the OR operation of both results in the time domain.

Figure 6 shows a profile of the BR and the HR obtained from measurements over a single night. The vertical axis denotes the BR/HR in units of breaths per minute or beats per minute (bpm). The black dots and vertical bars, terminated at the upper and lower ends by short horizontal lines, show the mean values and standard deviation on a beat-by-beat basis for the HR and a breath-by-breath basis for the BR for each minute. Discontinuities in the estimation of the BR/HR are denoted by the vertical bars occurring sporadically over time, and their widths denote periods of body movement. The broader vertical bars correspond to longer body movement periods.
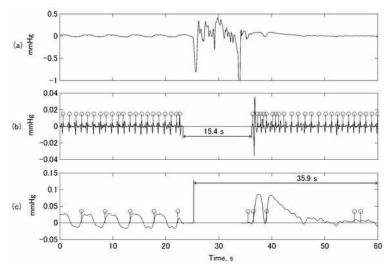
Fig. 5. An example of body movement in which both the BR and the HR are not fully detectable in a given period with different spans. The horizontal arrows indicate the body movement period in seconds. (a) Measured pressure signal distorted by body movements. (b) Reconstructed waveform and detected HR, as well as the detected body movement period. (c) Reconstructed waveform and detected BR as well as the detected body movement period.
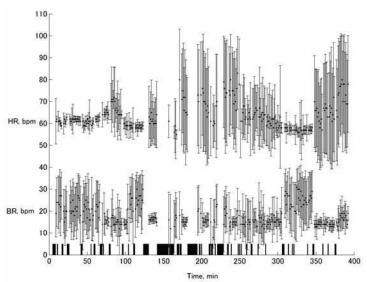


Fig. 6. Two profiles of the BR/HR obtained from measurements over a single night. The solid dots and vertical bars, terminated at the upper and lower ends by short horizontal lines, show the mean values and standard deviation within a period of one minute. The body movement periods are indicated by the variable-width vertical bars.

Figure 7 shows the complete profiles of the BR and HR during sleep over a period of 180 nights. The data were collected from a healthy female volunteer in her thirties at her own house over a period of seven months, under an informed agreement for the use of the data for research purposes. During this period, data over about 30 d were not measured. Therefore, data from a period of 180 d were recorded. The data are plotted on a day-by-day basis. The vertical axis represents the BR/HR in units of bpm. The symbols and vertical bars, terminated at the upper and lower ends by short horizontal lines, show the mean values and standard deviation of the detected HR (o) and the BR (*) in the corresponding night. The bold line is derived by filtering the mean values of the HR using a five-point Hanning window. The dashed line is an empirical estimate to indicate the possible trend of the average day base heart rate during those nights when data were not measured. Surprisingly, it is observed that the profile of the mean heart rate probably reveals a periodic property that corresponds to the female monthly menstrual cycle.
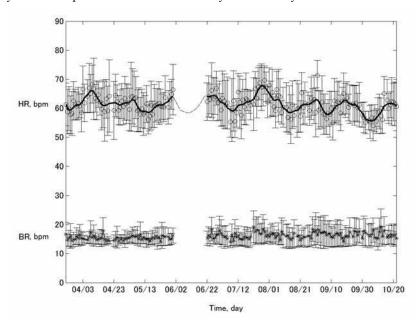


Fig. 7. Two complete profiles of the BR/HR over 180 nights. Data are plotted on a day-by-day basis. The symbols and vertical bars, terminated at the upper and lower ends by short horizontal lines, show the mean values and standard deviation of the detected HR (o) and the BR (*) in the corresponding night.

The devised system is completely invisible to the user during measurements. "Plug is all" is one of its significant characteristics in securing perpetuity in data collection. All a user has to do is just to plug in an AC power cable and a LAN cable. A user can even forget the existence of the device and perform no other operation once it is installed beneath a pillow on a bed. This property will substantially enhance its feasibility and usability in the home environment. A subtle variation in pressure under the pillow is detected as a first-order signal. The BR/HR and body movements are derived as second-order parameters. Sleep stage estimation, assessment of sleep quality, and biphasic menstrual cycle properties are third-

order parameters. In the end, a comprehensive interpretation of the multiple parameters obtained and a fully automatic operation property would increase its applicability in sleep lab studies, and also for screening patients who do not need a full sleep diagnosis at an early stage.

## 2.3 Wearable monitor for body temperature

Body temperature is one of the most important barometers indicating human health status. Moreover, the basal body temperature (BBT) is usually used for women to help estimate ovulation and to manage menstruation. However, a reliable evaluation of the menstrual cycle based on the BBT requires measurement of a woman's temperature under constant conditions for long periods. It is indeed a tedious task for a woman to measure her oral or armpit temperature under similar conditions when she wakes up every morning over a long period, because it usually takes an average of 5 min to measure temperature orally, or 10 min under the armpit. Moreover, the traditional method for evaluating ovulation or menstrual cycle dynamics in clinical practice is often based on a physician's empirical observations on serial measurements of BBT. It has been pointed out that the BBT failed to demonstrate ovulation in approximately 20% of ovulation cycles among 30 normally menstruating women (Moghissi, 1980). To improve user accessibility and the accuracy of the application of the BBT, we have developed a tiny wearable device for cutaneous temperature measurements and a Hidden Markov Model (HMM) based a statistical approach to estimate the biphasic properties of body temperature during the menstrual cycle using a series of cutaneous temperature data measured during sleep.

The wearable monitor can be attached to a woman's underwear or brassiere when asleep to measure the cutaneous temperature around the abdominal area or between the breasts, as shown in Fig. 8.
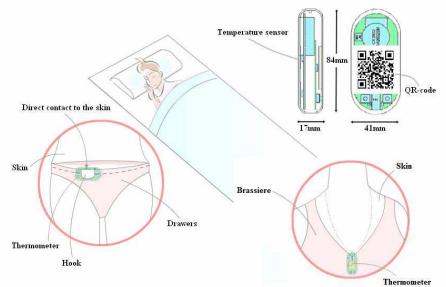


Fig. 8. A small, light wearable device (size = $41 \times 84 \times 17$ mm$^3$, weight = 59 g) for cutaneous temperature measurements during sleep (QOL Co. Ltd., 2008).

The device is programmed to measure temperature over 10 min intervals from midnight to 6 am. At most, 37 data points can be collected during the six hours. Outliers above 40 °C or below 32 °C are ignored. The collected temperature data are encoded in a two-dimensional bar code, known as "Quick Response" code (QR code) (Denso Wave Inc., 2000) and depicted on an LCD display. As shown in Fig. 9, the user uses the camera built into a mobile phone to capture the QR code image (a) on the device display (shown in the circle on the left-hand side of Fig. 9). Once the QR code is captured into the mobile phone (b), the original temperature data (c) are recovered from the captured image and transmitted to a database server via the mobile network for data storage and physiological interpretation through data mining.



Fig. 9. A procedure for temperature data collection using a wearable sensor and a mobile phone. (a) A QR code image. (b) A QR code captured by a camera built into a mobile phone. (c) Original data recovered from the image captured by a mobile phone (QOL Co. Ltd., 2008).

The temperature data measured during sleep over a six-month period are shown in Fig. 10(a). The nightly data are plotted in the vertical direction and have a range of 32 to 40 °C. The purpose of data mining in this study was to estimate the biphasic properties in the temperature profile during the menstrual cycle from cutaneous temperature measurements. As shown in Fig. 11, the biphasic properties of the menstrual cycle can be modelled as a discrete Hidden Markov Model (HMM) with two hidden phases. The measured temperature data are considered to be observations being generated by the Markov process from an unknown phase: either a low-temperature (LT) phase or a high-temperature (HT) phase, according to the probability distribution. The probability $b_L(k)$ is indicative that the value $k$ is generated from the hidden LT phase. The probability $b_H(k)$ is indicative that the value $k$ is generated from the hidden HT phase. The probability $a_{ii}$ is indicative of a hidden phase transition between LT and HT phases.
Figure 10(b) shows the results after pre-processing to removing outliers from the raw data and eliminating any discontinuities from non-data-collection days. Figure 10(c) shows the HMM estimation output using the pre-processed data from Fig. 10(b) as the input. Figure 10(d) shows the estimation of the biphasic properties after post-processing. The superimposed black symbols "*" denote the menstrual periods recorded by the user. A transition from the HT phase to the LT phase denotes a menstrual period, while the reverse transition denotes ovulation.
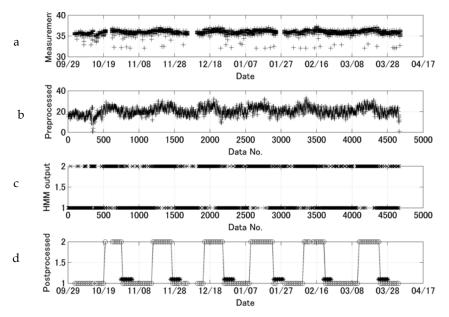
Fig. 10. Estimation procedure of a biphasic temperature profile. (a) Raw temperature data measured over a period of six months. (b) Pre-processed results. (c) Biphasic estimation based on an HMM approach. (d) Post-processed results. The symbol "*" denotes a menstrual period recorded by the user.
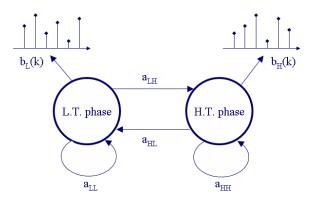


Fig. 11. A discrete hidden Markov model with two hidden phases for estimating biphasic property in a menstrual cycle from cutaneous temperature measurements.

The biphasic properties shown in Fig. 10(c) were estimated by finding an optimal HMM parameter set that determines the hidden phase from which each datum arises. This is based on a given series of measured temperature data, as shown in Fig. 10(b). The parameter set $\lambda(A,B,\pi)$ is assigned randomly in the initial condition and optimized through the forward–backward iterative procedure until $P(O|\lambda)$ converges to a stable maximum value or until the absolute logarithm of the previous and current difference in $P(O|\lambda)$ is not greater than $\delta$.

The algorithm for calculating the forward variable, α, the backward variable, β, and the forward–backward variable, γ, are shown in equations (2-3-1) to (2-3-3).

The forward variable, $\alpha_t(i)$, denotes the probability of phase, $q_i$, at time, $t$, based on a partial observation sequence, $O_1, O_2, \ldots, O_t$, until time $t$, and can be calculated using the following steps for a given set of λ(A,B,π).

$$\alpha_t(i) = P_r(O_1, O_2, \ldots, O_t, i_t = q_i \mid \lambda)$$

$$\alpha_1(i) = \pi_i b_i(O_1), \qquad 1 \le i \le N, t = 1$$

$$\alpha_{t+1}(j) = \left[ \sum_{i=1}^{N} \alpha_t(i) a_{ij} \right] b_j(O_{t+1}), \qquad 1 \le j \le N, t = 1, 2, \ldots, T-1 \tag{2-3-1}$$

The backward variable, $\beta_t(i)$, denotes the probability of phase, $q_i$, at time, $t$, based on a partial observation sequence, $O_{t+1}, O_{t+2}, \ldots, O_T$, from time $t+1$ to $T$, and can be calculated using the following steps for a given set of λ(A,B,π).

$$\beta_t(i) = P_r(O_{t+1}, O_{t+2}, \ldots, O_T \mid i_t = q_i, \lambda)$$

$$\beta_T(i) = 1, \qquad 1 \le i \le N, t = T$$

$$\beta_t(i) = \sum_{j=1}^{N} a_{ij} b_j(O_{t+1}) \beta_{t+1}(j), \qquad 1 \le i \le N, t = T-1, T-2, \ldots, 1 \tag{2-3-2}$$

To find the optimal sequence of hidden phases for a given observation sequence, $O$, and a given model, λ(A,B,π), there are multiple possible optimality criteria.

Choosing the phases, $q_t$, that are individually most likely at each time, $t$, i.e., maximizing $P(q_t = i \mid O, \lambda)$, is equivalent to finding the single best phase sequence (path), i.e., maximizing $P(Q \mid O, \lambda)$ or $P(Q, O \mid \lambda)$. The forward–backward algorithm is applied to find the optimal sequence of phases, $q_t$, at each time, $t$, i.e., to maximize $\gamma_t(i) = P(q_t = i \mid O, \lambda)$ for a given observation sequence, $O$, and a given set of λ(A,B,π).

$$\gamma_t(i) = P(q_t = i \mid O, \lambda)$$

$$= \frac{P(O, q_t = i \mid \lambda)}{P(O \mid \lambda)} = \frac{P(O, q_t = i \mid \lambda)}{\sum\limits_{i=1}^{N} P(O, q_t = i \mid \lambda)}$$

$$= \frac{P(o_1 o_2 \ldots o_t, q_t = i \mid \lambda) P(o_{t+1} o_{t+2} \ldots o_T \mid q_t = i, \lambda)}{\sum\limits_{i=1}^{N} P(o_1 o_2 \ldots o_t, q_t = i \mid \lambda) P(o_{t+1} o_{t+2} \ldots o_T \mid q_t = i, \lambda)} \tag{2-3-3}$$

$$= \frac{\alpha_t(i) \beta_t(i)}{\sum\limits_{i=1}^{N} \alpha_t(i) \beta_t(i)}$$

The most likely phase, $q_t$* at time $t$ can be found as:

$$q_t^* = \arg\max_{1 \le i \le N} \left[ \gamma_t(i) \right], \qquad 1 \le t \le T . \tag{2-3-4}$$

As there are no existing analytical methods for optimizing $\lambda(A,B,\pi)$, $P(O|\lambda)$ or $P(O,I|\lambda)$ is usually maximized (i.e., $\lambda^* = \arg\max_\lambda [P(O|\lambda)]$ or $\lambda^* = \arg\max_\lambda [P(O,Q|\lambda)]$) using gradient techniques and an expectation-maximization method. In this study, the Baum–Welch method was used because of its numerical stability and linear convergence (Rabiner, 1989).

To update $\lambda(A,B,\pi)$ using the Baum–Welch re-estimation algorithm, we defined a variable, $\xi_t(i,j)$, to express the probability of a datum being in phase $i$ at time $t$ and phase $j$ at time $t+1$, given the model and the observation sequence:

$$\xi_t(i,j) = P\left(q_t = i, q_{t+1} = j \mid O, \lambda\right) = \frac{P\left(q_t = i, q_{t+1} = j, O \mid \lambda\right)}{P(O \mid \lambda)}. \tag{2-3-5}$$

From the definitions of the forward and backward variables, $\xi_t(i,j)$ and $\gamma_t(i)$, can be related as:

$$\xi_t(i,j) = \frac{\alpha_t(i) a_{ij} b_j(o_{t+1}) \beta_{t+1}(j)}{P(O \mid \lambda)} = \frac{\alpha_t(i) a_{ij} b_j(o_{t+1}) \beta_{t+1}(j)}{\sum_{i=1}^{N} \sum_{j=1}^{N} \alpha_t(i) a_{ij} b_j(o_{t+1}) \beta_{t+1}(j)}, \tag{2-3-6}$$

$$\gamma_t(i) = P\left(q_t = i \mid O, \lambda\right) = \sum_{j=1}^{N} P\left(q_t = i, q_{t+1} = j \mid O, \lambda\right) = \sum_{j=1}^{N} \xi_t(i,j), \tag{2-3-7}$$

where $\sum_{t=1}^{T-1} \gamma_t(i)$ denotes the expected number of transitions from phase $i$ in $O$. The term $\sum_{t=1}^{T-1} \xi_t(i,j)$ denotes the expected number of transitions from phase $i$ to phase $j$ in $O$.

Therefore, $\lambda(A,B,\pi)$ can be updated using equations (2-3-8) to (2-3-10) as follows.

As $\pi_i$ is the initial probability and denotes the expected frequency (number of times) in phase $i$ at time $t = 1$ as $\pi_i = \gamma_1(i)$, it can be calculated using the forward and backward variables.

$$\pi_i = \frac{\alpha_1(i)\beta_1(i)}{\sum_{i=1}^{N} \alpha_1(i)\beta_1(i)} = \frac{\alpha_1(i)\beta_1(i)}{\sum_{i=1}^{N} \alpha_T(i)}, \tag{2-3-8}$$

The transition probability from phase $i$ to phase $j$, $a_{ij}$, can be calculated from the expected number of transitions from phase $i$ to phase $j$ divided by the expected number of transitions from phase $i$.

$$a_{ij} = \frac{\sum_{t=1}^{T-1} \xi_t(i,j)}{\sum_{t=1}^{T-1} \gamma_t(i)} = \frac{\sum_{t=1}^{T-1} \alpha_t(i) a_{ij} b_j(o_{t+1}) \beta_{t+1}(j)}{\sum_{t=1}^{T-1} \alpha_t(i)\beta_t(i)}, \tag{2-3-9}$$

# Thank You for previewing this eBook

You can read the full version of this eBook in different formats:

> ➢ HTML (Free /Available to everyone)

> ➢ PDF / TXT (Available to V.I.P. members. Free Standard members can access up to 5 PDF/TXT eBooks per month each month)

> ➢ Epub & Mobipocket (Exclusive to V.I.P. members)

To download this full book, simply select the format you desire below